

A model of relative position and attitude in a leader-follower spacecraft formation

Raymond Kristiansen*, Esten Ingar Grøtli**, Per Johan Nicklasson*
and Jan Tommy Gravdahl**

*Department of Space Technology
Narvik University College, Norway

**Department of Engineering Cybernetics
Norwegian University of Science and Technology, Norway

Abstract

In this paper, a model of a leader-follower spacecraft formation in six degrees of freedom is derived and presented. The nonlinear model describes the relative translational and rotational motion of the spacecraft, and extends previous work by providing a more complete factorization, together with detailed information about the matrices in the model. In addition, mathematical models of orbital perturbations due to gravitational variations, atmospheric drag, solar radiation and third-body effects are derived. Results from simulations are presented to visualize the properties of the model and to show the impact of the different disturbances on the flight path.

1 Introduction

1.1 Background

The concept of flying spacecraft in formation is revolutionizing our way of performing space-based operations, and this new paradigm brings out several advantages in space mission accomplishment and extends the possible application area for such systems. Earth and deep space surveillance are areas where spacecraft formations can be useful. These applications often involve data collection and processing over an aperture where the resolution of the observation is inversely proportional to the baseline lengths. Further exploration of neighboring galaxies in space can only be achieved by indirect observation of astronomical objects, and space based interferometers with baselines of up to ten kilometers have been proposed. However, to successfully utilize spacecraft formations for this purpose, accurate synchronization of both position

and attitude of the cooperating spacecraft is vital, depending on accurate dynamical system models of the formation.

1.2 Previous work

The simplest model of relative motion between two spacecraft is linear and multi-variable, and known as the Hill [1] or Clohessy-Wiltshire equations [2]. This model originated from the equations of the two-body problem, based on the laws of Newton and Kepler, and has inherently assumptions that the orbit is circular with no orbital perturbations, and that the distance between spacecraft is small relative to the distance from the formation to the center of the Earth. An extension to elliptic Keplerian orbits, yet still assuming no orbital perturbations, is what is known as the Lawden equations [3] or also Tschauner-Hempel equations [4]. Both models were originally presented for solutions of the problem of orbital rendezvous, but has been adopted later for the very similar and more general spacecraft formation flying control problem. Some years later, nonlinear models as presented in e.g. [5, 6, 7] were derived for arbitrary orbital eccentricity and with added terms for orbital perturbations.

Models of both translational and rotational motion in a leader-follower spacecraft formation have been considered by few researchers, and most of the previous work has focused on translational models only. However, notable exceptions are [8, 9], where models of coupled translational and rotational motion were derived. In [10], a 6DOF model based on orbit element differences was derived, to develop an integrated control system for attitude and orbit control. A coordinate-free model of translation and rotation for a single spacecraft in a formation was presented in sev-

eral different forms in [11]. None of these results included models of environmental disturbances.

1.3 Contribution

This paper presents a detailed nonlinear mathematical model in six degrees of freedom of relative translation and rotation of two spacecraft in a leader-follower formation, which is well suited for control. The model of relative position is based on the two-body equations derived from Newton's inverse square law of gravity, and extends previous work by providing a more complete factorization, together with detailed information about the matrices in the model. The position and velocity vectors of the follower spacecraft are represented in a coordinate reference frame located in the center of mass of the leader spacecraft, known as the Hill frame. The relative attitude model is based on Euler's momentum equations, and the attitude is represented by unit quaternions and angular velocities.

The model also includes the mathematical expressions for external disturbances originating from gravitational variations, atmospheric drag, solar radiation, and perturbations due to other celestial bodies, known as third body effects.

The rest of the paper is organized as follows: Section 2 describes the reference coordinate frames used in the paper, and matrices for vector rotation between frames. In Section 3 the model of relative position and velocity is derived, and the model of relative attitude and angular velocity is derived in Section 4. Expressions for orbital perturbations are given in Section 5. Simulation results for a spacecraft formation are presented in Section 6, and concluding remarks can be found in Section 7.

2 Coordinate frames

2.1 Cartesian coordinate frames

The coordinate reference frames used throughout the paper are given in Figure 1 and defined as follows:

Earth Centered Inertial (ECI) frame: This frame is denoted \mathcal{F}_i , and has its origin located in the center of the Earth. Its z axis is directed along the rotation axis of the Earth towards the celestial north pole, the x axis is directed towards the vernal equinox, and finally the direction of the y axis completes a right handed orthogonal frame.

Leader orbit reference frame: The leader orbit frame, denoted \mathcal{F}_l , has its origin located in the center of mass of the leader spacecraft. The \mathbf{e}_r axis in

the frame is parallel to the vector \mathbf{r}_l pointing from the center of the Earth to the spacecraft, and the \mathbf{e}_h axis is parallel to the orbit momentum vector, which points in the orbit normal direction. The \mathbf{e}_θ axis completes the right-handed orthogonal frame. The basis vectors of

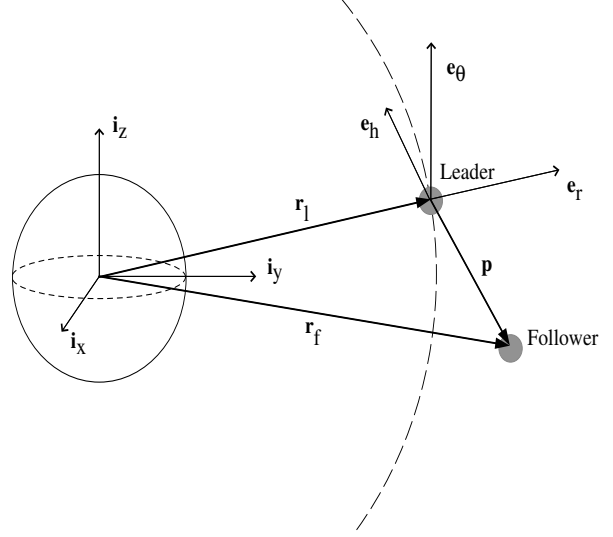


Figure 1: Reference coordinate frames [12].

the frame can be defined as

$$\mathbf{e}_r = \frac{\mathbf{r}_l}{r_l} \quad \mathbf{e}_\theta = \mathbf{e}_h \times \mathbf{e}_r \quad \mathbf{e}_h = \frac{\mathbf{h}}{h}$$

where $\mathbf{h} = \mathbf{r}_l \times \dot{\mathbf{r}}_l$ is the angular momentum vector of the orbit, and $h = |\mathbf{h}|$.

In addition to the basis vectors of the frame \mathcal{F}_l , two auxiliary vectors \mathbf{e}_v and \mathbf{e}_n are defined, as shown in Figure 2. The first vector \mathbf{e}_v is pointing along the spacecraft velocity vector, while \mathbf{e}_n is defined to be orthogonal to \mathbf{e}_v and \mathbf{e}_h , as $\mathbf{e}_n = \mathbf{e}_v \times \mathbf{e}_h$. If the spacecraft orbit is circular, then $\mathbf{e}_v = \mathbf{e}_\theta$ and $\mathbf{e}_n = \mathbf{e}_r$.

Follower orbit reference frame: This frame has its origin in the center of mass of the follower spacecraft, and is denoted \mathcal{F}_f . The vector pointing from the center of the Earth to the center of the follower orbit frame is denoted \mathbf{r}_f . Its origin is specified by a relative orbit position vector $\mathbf{p} = [x \ y \ z]^T$ expressed in \mathcal{F}_l frame components, as shown in Figure 1, and the frame unit vectors align with the basis vectors of \mathcal{F}_l . Accordingly,

$$\mathbf{p} = \mathbf{r}_f - \mathbf{r}_l = x\mathbf{e}_r + y\mathbf{e}_\theta + z\mathbf{e}_h \quad (1)$$

Body reference frames: For both the leader and the follower spacecraft, body reference frames are defined and denoted \mathcal{F}_{bl} and \mathcal{F}_{bf} , respectively. These frames have, similar to the orbit frame, the origin located in

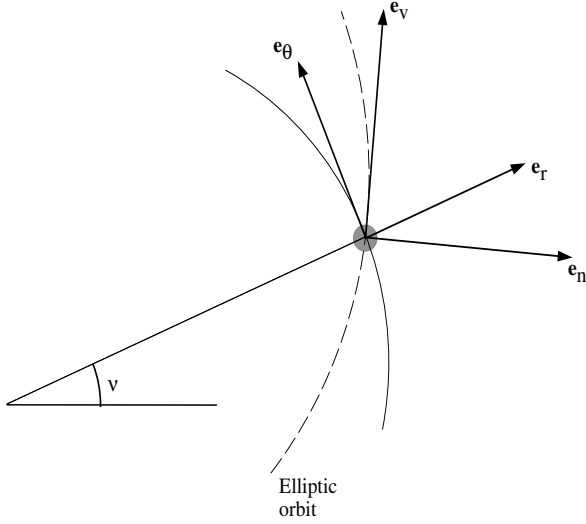


Figure 2: Auxiliary vectors for the leader orbit reference frame [12].

the center of mass of the respective spacecraft, but the basis vectors are fixed in the spacecraft body and coincide with its principal axis of inertia.

2.2 Coordinate frame transformations

2.2.1 Rotation from ECI to leader orbit frame

The rotation from the ECI frame to the leader orbit frame is dependent on the parameters of the leader spacecraft orbit, and can be expressed by three consecutive rotations. The total rotation matrix can be written

$$\mathbf{R}_i^l = \mathbf{R}_{z,\omega+\nu} \mathbf{R}_{x,i} \mathbf{R}_{z,\Omega}$$

where Ω is the right ascension of the ascending node of the orbit, i is the inclination of the orbit, ν is the true anomaly of the leader orbit, and ω is the argument of perigee of the same. The sum of ν and ω represents the location of the spacecraft relative to the ascending node.

2.2.2 Orbit frame transformation

Using both the original and the auxiliary vectors in the orbit frame, as shown in Figure 2, spacecraft acceleration can be written as

$$\mathbf{a} = a_r \mathbf{e}_r + a_\theta \mathbf{e}_\theta + a_h \mathbf{e}_h = a_n \mathbf{e}_n + a_v \mathbf{e}_v + a_h \mathbf{e}_h \quad (2)$$

The spacecraft velocity vector can be expressed as [12]

$$\mathbf{v} = \dot{\mathbf{r}} = \frac{\mu}{h} \left(e \sin \nu \mathbf{e}_r + \frac{p}{r} \mathbf{e}_\theta \right)$$

where μ is the geocentric gravitational constant of the Earth, h is the magnitude of angular momentum, e is the eccentricity and $p = h^2/\mu$ is the semi-latus rectum of the spacecraft orbit. Therefore, since \mathbf{e}_v is pointing along the velocity vector,

$$\mathbf{e}_v = \frac{\mathbf{v}}{v} = \frac{h}{pv} \left(e \sin \nu \mathbf{e}_r + \frac{p}{r} \mathbf{e}_\theta \right) \quad (3)$$

Moreover, since \mathbf{e}_n is defined normal to \mathbf{e}_v and \mathbf{e}_h ,

$$\mathbf{e}_n = \mathbf{e}_v \times \mathbf{e}_h = \frac{h}{pv} \left(\frac{p}{r} \mathbf{e}_r - e \sin \nu \mathbf{e}_\theta \right) \quad (4)$$

The transformation between the orbit plane acceleration vector components can now be found from (2), (3) and (4) as

$$\begin{bmatrix} a_r \\ a_\theta \end{bmatrix} = \frac{h}{pv} \begin{bmatrix} \frac{p}{r} & e \sin \nu \\ -e \sin \nu & \frac{p}{r} \end{bmatrix} \begin{bmatrix} a_n \\ a_v \end{bmatrix}$$

so that

$$\mathbf{C}_a^l = \frac{h}{pv} \begin{bmatrix} \frac{p}{r} & e \sin \nu & 0 \\ -e \sin \nu & \frac{p}{r} & 0 \\ 0 & 0 & \frac{pv}{h} \end{bmatrix} \quad (5)$$

Note that \mathbf{C}_a^l is not a proper rotation matrix since

$$\det \mathbf{C}_a^l = 1 + e^2 + 2e \cos \nu \quad (6)$$

2.2.3 Body frame rotation

The rotation matrix describing rotations from an orbit frame to a body frame can be described by

$$\mathbf{R}_o^b = (\mathbf{c}_1 \ \mathbf{c}_2 \ \mathbf{c}_3) = \mathbf{I} + 2\eta \mathbf{S}(\boldsymbol{\varepsilon}) + 2\mathbf{S}^2(\boldsymbol{\varepsilon}) \quad (7)$$

where the elements \mathbf{c}_i are directional cosines, and

$$\mathbf{q} = [\ \eta \quad \boldsymbol{\varepsilon}^T \]^T \quad (8)$$

are the Euler parameters. The inverse rotation is given by the complex conjugate of \mathbf{q} as

$$\bar{\mathbf{q}} = [\ \eta \quad -\boldsymbol{\varepsilon}^T \]^T$$

3 Translational motion

3.1 The N-body problem

Consider a system of N bodies with masses m_i , $i = 1, 2, \dots, N$. The position and velocity vectors of the i 'th mass relative to the ECI frame are defined as \mathbf{r}_i and \mathbf{v}_i respectively, where $\mathbf{r}_i = x_i \mathbf{i}_x + y_i \mathbf{i}_y + z_i \mathbf{i}_z$ and $\mathbf{v}_i = \frac{d\mathbf{r}_i}{dt}$.

The distance between any two particles with mass m_i and m_j is denoted by

$$r_{ij} = |\mathbf{r}_j - \mathbf{r}_i|$$

and the magnitude of the force of attraction between the masses is $Gm_i m_j / r_{ij}^2$ where G is the universal constant of gravity [13]. The direction of the forces are expressed in terms of unit vectors, and the force acting on m_i due to m_j has the direction $(\mathbf{r}_j - \mathbf{r}_i) / r_{ij}$, while the force on m_j due to m_i has the opposite direction. The force \mathbf{f}_i acting on mass m_i due to all the other $N - 1$ masses can be expressed as

$$\mathbf{f}_i = G \sum_{j=1}^n \frac{m_i m_j}{r_{ij}^3} (\mathbf{r}_j - \mathbf{r}_i), \quad i, j = 1, 2, \dots, N, \quad i \neq j$$

and application of Newton's second law of motion yields N vector differential equations

$$\frac{d^2 \mathbf{r}_i}{dt^2} = G \sum_{j=1}^n \frac{m_j}{r_{ij}^3} (\mathbf{r}_j - \mathbf{r}_i), \quad i \neq j \quad (9)$$

Together with appropriate initial conditions, this constitutes a complete mathematical description of the motion of a system of N bodies. From this relation, the fundamental differential equation of the two-body problem can be found as [13]

$$\frac{d^2 \mathbf{r}}{dt^2} + \frac{\mu}{r^3} \mathbf{r} = \mathbf{0} \quad (10)$$

where $\mathbf{r} = \mathbf{r}_2 - \mathbf{r}_1$ is the relative position of masses and $\mu = G(m_1 + m_2)$.

3.2 Formation dynamics

The general orbit equation (10) is the equation describing the orbit dynamics for a spacecraft under ideal conditions, i.e. with no external disturbances. This equation can be generalized to include force terms due to aerodynamic disturbances, gravitational forces from other bodies, solar radiation, magnetic fields and so on. In addition, it can be augmented to include control input vectors from onboard actuators. Accordingly, (10) can be expressed for the leader and follower spacecraft as

$$\begin{aligned} \ddot{\mathbf{r}}_l &= -\frac{\mu}{r_l^3} \mathbf{r}_l - \frac{\mathbf{f}_{dl}}{m_l} + \frac{\mathbf{u}_l}{m_l} \\ \ddot{\mathbf{r}}_f &= -\frac{\mu}{r_f^3} \mathbf{r}_f - \frac{\mathbf{f}_{df}}{m_f} + \frac{\mathbf{u}_f}{m_f} \end{aligned}$$

where $\mathbf{f}_{dl}, \mathbf{f}_{df} \in \mathbb{R}^3$ are the disturbance terms due to external effects and $\mathbf{u}_l, \mathbf{u}_f \in \mathbb{R}^3$ are the actuator

forces of the leader and follower spacecraft, respectively. The second order derivative of the relative position vector can now be expressed as

$$\begin{aligned} \ddot{\mathbf{p}} &= \ddot{\mathbf{r}}_f - \ddot{\mathbf{r}}_l \\ &= -\frac{\mu}{r_f^3} \mathbf{r}_f - \frac{\mathbf{f}_{df}}{m_f} + \frac{\mathbf{u}_f}{m_f} + \frac{\mu}{r_l^3} \mathbf{r}_l + \frac{\mathbf{f}_{dl}}{m_l} - \frac{\mathbf{u}_l}{m_l} \end{aligned}$$

so that

$$\begin{aligned} m_f \ddot{\mathbf{p}} &= -m_f \mu \left(\frac{\mathbf{r}_l + \mathbf{p}}{(r_l + p)^3} - \frac{\mathbf{r}_l}{r_l^3} \right) \\ &\quad + \mathbf{u}_f - \mathbf{f}_{df} - \frac{m_f}{m_l} (\mathbf{u}_l - \mathbf{f}_{dl}) \end{aligned} \quad (11)$$

On the other hand, from (1), the inertial position equation for the follower spacecraft can be expressed as

$$\mathbf{r}_f = \mathbf{r}_l + \mathbf{p} = (r_l + x) \mathbf{e}_r + y \mathbf{e}_\theta + z \mathbf{e}_h$$

Differentiation of this equation twice with respect to time leaves

$$\begin{aligned} \ddot{\mathbf{r}}_f &= (\ddot{r}_l + \ddot{x}) \mathbf{e}_r + 2(\dot{r}_l + \dot{x}) \dot{\mathbf{e}}_r + (r_l + x) \ddot{\mathbf{e}}_r \\ &\quad + \ddot{y} \mathbf{e}_\theta + 2\dot{y} \dot{\mathbf{e}}_\theta + y \ddot{\mathbf{e}}_\theta + \ddot{z} \mathbf{e}_h + 2\dot{z} \dot{\mathbf{e}}_h + z \ddot{\mathbf{e}}_h \end{aligned} \quad (12)$$

By using the true anomaly v of the leader spacecraft, the relationships

$$\dot{\mathbf{e}}_r = \dot{v} \mathbf{e}_\theta \quad \dot{\mathbf{e}}_\theta = -\dot{v} \mathbf{e}_r \quad (13)$$

$$\ddot{\mathbf{e}}_r = \ddot{v} \mathbf{e}_\theta - \dot{v}^2 \mathbf{e}_r \quad \ddot{\mathbf{e}}_\theta = -\ddot{v} \mathbf{e}_r - \dot{v}^2 \mathbf{e}_\theta \quad (14)$$

can be found. Insertion of (13)-(14) into (12), while recognizing that no out-of-plane motion exists, and hence $\dot{\mathbf{e}}_h = \ddot{\mathbf{e}}_h = \mathbf{0}$, gives

$$\begin{aligned} \ddot{\mathbf{r}}_f &= (\ddot{r}_l + \ddot{x} - 2\dot{y}\dot{v} - \dot{v}^2(r_l + x) - y\ddot{v}) \mathbf{e}_r \\ &\quad + (\ddot{y} + 2\dot{v}(\dot{r}_l + \dot{x}) + \ddot{v}(r_l + x) - y\dot{v}^2) \mathbf{e}_\theta + \ddot{z} \mathbf{e}_h \end{aligned} \quad (15)$$

Moreover, the position of the leader spacecraft can be expressed as

$$\mathbf{r}_l = r_l \mathbf{e}_r \quad (16)$$

Differentiating (16) twice with respect to time and inserting (13)-(14), results in

$$\begin{aligned} \ddot{\mathbf{r}}_l &= \ddot{r}_l \mathbf{e}_r + 2\dot{r}_l \dot{\mathbf{e}}_r + r_l \ddot{\mathbf{e}}_r \\ &= (\ddot{r}_l - r_l \dot{v}^2) \mathbf{e}_r + (2\dot{r}_l \dot{v} + r_l \ddot{v}) \mathbf{e}_\theta \end{aligned} \quad (17)$$

Subtracting (17) from (15) results in one other formulation for the position vector acceleration:

$$\begin{aligned} \ddot{\mathbf{p}} &= \ddot{\mathbf{r}}_f - \ddot{\mathbf{r}}_l \\ &= (\ddot{x} - 2\dot{y}\dot{v} - \dot{v}^2 x - \dot{v} y) \mathbf{e}_r \\ &\quad + (\ddot{y} + 2\dot{v}\dot{x} + \dot{v}x - \dot{v}^2 y) \mathbf{e}_\theta + \ddot{z} \mathbf{e}_h \end{aligned} \quad (18)$$

Substituting (18) into (11) leaves the nonlinear position dynamics on the form

$$m_f \ddot{\mathbf{p}} + \mathbf{C}(\dot{\mathbf{v}}) \dot{\mathbf{p}} + \mathbf{D}(\dot{\mathbf{v}}, \ddot{\mathbf{v}}, r_l) \mathbf{p} + \mathbf{n}(r_l, r_f) = \mathbf{U} - \mathbf{F}_d$$

similar to the one derived in [7], where

$$\mathbf{C}(\dot{\mathbf{v}}) = 2m_f \dot{\mathbf{v}} \begin{bmatrix} 0 & -1 & 0 \\ 1 & 0 & 0 \\ 0 & 0 & 0 \end{bmatrix}$$

is the skew-symmetric Coriolis-like matrix, which thus is a member of the special symmetrical group $SS(3)$, and hence

$$\mathbf{C}(\dot{\mathbf{v}}) + \mathbf{C}^T(\dot{\mathbf{v}}) = \mathbf{0}$$

Furthermore,

$$\mathbf{D}(\dot{\mathbf{v}}, \ddot{\mathbf{v}}, r_l) = m_f \begin{bmatrix} \frac{\mu}{r_f^3} - \dot{\mathbf{v}}^2 & -\ddot{\mathbf{v}} & 0 \\ \ddot{\mathbf{v}} & \frac{\mu}{r_f^3} - \dot{\mathbf{v}}^2 & 0 \\ 0 & 0 & \frac{\mu}{r_f^3} \end{bmatrix} \quad (19)$$

and

$$\mathbf{n}(r_l, r_f) = m_f \mu \begin{bmatrix} \frac{r_l}{r_f^3} - \frac{1}{r_l^2} \\ 0 \\ 0 \end{bmatrix}$$

The composite disturbance force \mathbf{F}_d is given by

$$\mathbf{F}_d = \mathbf{f}_{df} - \frac{m_f}{m_l} \mathbf{f}_{dl}$$

and the relative control force \mathbf{U} is given by

$$\mathbf{U} = \mathbf{u}_f - \frac{m_f}{m_l} \mathbf{u}_l$$

Moreover, the eigenvalues of the matrix $\mathbf{D}(\dot{\mathbf{v}}, \ddot{\mathbf{v}}, r_l)$ in (19) are

$$\begin{aligned} \lambda_1 &= \frac{\mu}{r_f^3} + \ddot{\mathbf{v}} - \dot{\mathbf{v}}^2 \\ \lambda_2 &= \frac{\mu}{r_f^3} - \ddot{\mathbf{v}} - \dot{\mathbf{v}}^2 \\ \lambda_3 &= \frac{\mu}{r_f^3} \end{aligned} \quad (20)$$

so it can be shown that $\mathbf{D}(\dot{\mathbf{v}}, \ddot{\mathbf{v}}, r_l) > 0$ when

$$r_f^3 < \frac{a^3 (1 - e^2)^3}{(1 + e \cos \nu)^4} \quad (21)$$

where a is the semimajor axis of the leader orbit. If the orbit of the leader spacecraft is circular, then $e = 0$ and (21) reduces to $r_f < a$, so $\mathbf{D}(\dot{\mathbf{v}}, \ddot{\mathbf{v}}, r_l) > 0$ when the follower is located within the circle with origin in the center of the Earth and radius a . At the other end, when the leader orbit tends towards an parabolic orbit, then $e \rightarrow 1$ and (21) reduces to $r_f < 0$, which is practically infeasible.

4 Rotational motion

4.1 Attitude kinematics

The time derivative of a matrix \mathbf{R}_b^a as in (7) can according to [14] be written as

$$\dot{\mathbf{R}}_b^a = \mathbf{S}(\omega_{a,b}^a) \mathbf{R}_b^a = \mathbf{R}_{bS}^a(\omega_{a,b}^b) \quad (22)$$

where $\omega_{a,b}^b$ is the angular velocity of frame b relative to frame a represented in frame b and $\mathbf{S}(\cdot)$ is the cross product operator given by

$$\mathbf{S}(\omega) = \omega \times = \begin{bmatrix} 0 & -\omega_3 & \omega_2 \\ \omega_3 & 0 & -\omega_1 \\ -\omega_2 & \omega_1 & 0 \end{bmatrix}$$

when ω is an arbitrary vector in three dimensions given by $\omega = [\omega_1 \ \omega_2 \ \omega_3]^T$. The kinematic differential equations for a spacecraft in its orbit frame can be found from (22) together with (8) as

$$\dot{\mathbf{q}}_s = \begin{bmatrix} \dot{\eta}_s \\ \dot{\epsilon}_s \end{bmatrix} = \frac{1}{2} \begin{bmatrix} -\epsilon_s^T \\ \eta_s \mathbf{I} + \mathbf{S}(\epsilon_s) \end{bmatrix} \omega_{s, sb}^{sb} \quad (23)$$

where $\omega_{s, sb}^{sb}$ is the angular velocity of the spacecraft body frame relative to the orbit frame, referenced in the body frame. The superscript/subscript s is used in general to denote the spacecraft in question, so $s = l, f$ for the leader and follower spacecraft, respectively.

4.2 Attitude dynamics

With the assumptions of rigid body movement, the dynamical model of a spacecraft can be found from Euler's momentum equation as [15]

$$\mathbf{J}_s \dot{\omega}_{i, sb}^{sb} = -\mathbf{S}(\omega_{i, sb}^{sb}) \mathbf{J}_l \omega_{i, sb}^{sb} + \tau_d^{sb} + \tau_a^{sb} \quad (24)$$

$$\omega_{s, sb}^{sb} = \omega_{i, sb}^{sb} + \omega_o \mathbf{c}_2 \quad (25)$$

where \mathbf{J}_s is the spacecraft inertia matrix and $\omega_{i, sb}^{sb}$ is the angular velocity of the spacecraft body frame relative to the inertial frame, expressed in the body frame. The parameter ω_o is the orbit angular velocity, τ_d^{sb} is the total disturbance torque, τ_a^{sb} is the actuator torque, and \mathbf{c}_2 is the directional cosine vector from (7).

4.3 Relative attitude

By expressing the relations in (23) and (24)-(25) for both the leader and the follower spacecraft, and utilizing the quaternion product defined in [14] as

$$\mathbf{q} = \mathbf{q}_f \otimes \bar{\mathbf{q}}_l \triangleq \begin{bmatrix} \eta_f \eta_l + \epsilon_f^T \epsilon_l \\ \eta_f \epsilon_l - \eta_l \epsilon_f - \mathbf{S}(\epsilon_f) \epsilon_l \end{bmatrix}$$

the relative attitude kinematics and dynamics can be expressed as [16]

$$\dot{\mathbf{q}} = \begin{bmatrix} \dot{\boldsymbol{\eta}} \\ \dot{\boldsymbol{\varepsilon}} \end{bmatrix} = \frac{1}{2} \begin{bmatrix} -\boldsymbol{\varepsilon}^T \\ \boldsymbol{\eta}\mathbf{I} + \mathbf{S}(\boldsymbol{\varepsilon}) \end{bmatrix} \boldsymbol{\omega}$$

where

$$\boldsymbol{\omega} = \boldsymbol{\omega}_{i,fb}^{fb} - \mathbf{R}_{lb}^{fb} \boldsymbol{\omega}_{i,lb}^{lb} \quad (26)$$

is the relative angular velocity between the leader body reference frame and the follower body reference frame. Moreover, from (26) the relative attitude dynamics can be expressed as

$$\begin{aligned} \mathbf{J}_f \dot{\boldsymbol{\omega}} &= \mathbf{J}_f \dot{\boldsymbol{\omega}}_{i,fb}^{fb} - \mathbf{J}_f \dot{\mathbf{R}}_{lb}^{fb} \boldsymbol{\omega}_{i,lb}^{lb} - \mathbf{J}_f \mathbf{R}_{lb}^{fb} \dot{\boldsymbol{\omega}}_{i,lb}^{lb} \\ &= \mathbf{J}_f \dot{\boldsymbol{\omega}}_{i,fb}^{fb} - \mathbf{J}_f \mathbf{S} \left(\boldsymbol{\omega}_{i,lb}^{fb} \right) \boldsymbol{\omega} - \mathbf{J}_f \mathbf{R}_{lb}^{fb} \dot{\boldsymbol{\omega}}_{i,lb}^{lb} \end{aligned} \quad (27)$$

where (22) and the facts that $\boldsymbol{\omega}_{lb,fb}^{fb} = \boldsymbol{\omega}$ and $\mathbf{S}(\mathbf{a})\mathbf{b} = -\mathbf{S}(\mathbf{b})\mathbf{a}$ has been used. Insertion of (24), evaluated for both the leader and follower, into (27) results in

$$\begin{aligned} \mathbf{J}_f \dot{\boldsymbol{\omega}} &= -\mathbf{S} \left(\boldsymbol{\omega} + \mathbf{R}_{lb}^{fb} \boldsymbol{\omega}_{i,lb}^{lb} \right) \mathbf{J}_f \left(\boldsymbol{\omega} + \mathbf{R}_{lb}^{fb} \boldsymbol{\omega}_{i,lb}^{lb} \right) \\ &\quad + \mathbf{J}_f \mathbf{R}_{lb}^{fb} \mathbf{J}_l^{-1} \mathbf{S} \left(\boldsymbol{\omega}_{i,lb}^{lb} \right) \mathbf{J}_l \boldsymbol{\omega}_{i,lb}^{lb} \\ &\quad - \mathbf{J}_f \mathbf{S} \left(\mathbf{R}_{lb}^{fb} \boldsymbol{\omega}_{i,lb}^{lb} \right) \boldsymbol{\omega} + \Upsilon_d + \Upsilon_a \end{aligned}$$

where

$$\Upsilon_d = \boldsymbol{\tau}_d^{fb} - \mathbf{J}_f \mathbf{R}_{lb}^{fb} \mathbf{J}_l^{-1} \boldsymbol{\tau}_d^{lb}$$

and

$$\Upsilon_a = \boldsymbol{\tau}_a^{fb} - \mathbf{J}_f \mathbf{R}_{lb}^{fb} \mathbf{J}_l^{-1} \boldsymbol{\tau}_a^{lb}$$

are the relative disturbance torques and relative actuator torques, respectively.

5 Orbital perturbations

Spacecraft flying in a Keplerian orbit will be subject to accelerations caused by minor disturbances. Some of the sources for these disturbances are gravitational attractions from celestial bodies, non-spherical shapes of planets, atmospheric drag, or solar radiation pressure [12]. The resulting expressions for these perturbations are in the following derived generally for a spacecraft in Earth orbit, without relating to leader or follower spacecraft.

5.1 Perturbing forces

5.1.1 Atmospheric drag

At altitudes lower than approximately 500 km, Earth atmosphere is so dense that the resulting aerodynamic drag has a considerable impact on spacecraft orbits [17]. The aerodynamic force can be written as

$$\mathbf{f}_{atm}^s = \mathbf{C}_a^s \begin{bmatrix} 0 \\ \frac{1}{2} \rho V^2 C_d A \\ 0 \end{bmatrix} \quad (28)$$

where ρ is the atmospheric density, V is the spacecraft velocity in the direction of the \mathbf{e}_v vector depicted in Figure 2, C_d is the drag coefficient, A is the equivalent spacecraft surface in the direction of motion of the spacecraft and \mathbf{C}_a^s denotes the orbit frame transformation matrix, as described in (5). The superscript s is used for generality to indicate the orbit frame for the inflicted spacecraft.

5.1.2 Solar radiation and solar wind

Radiation and particles expelled from the Sun will affect the spacecraft orbit independent of the spacecraft altitude [17]. The disturbance force from solar radiation is dependent on the reflectance of the spacecraft material, and consists of absorption, specular reflection and diffuse reflection. The surfaces of a spacecraft is usually non-diffuse, and the reflection is a combination of absorption and specular reflection. The diffuse reflection is hence neglected in the further analysis. A visualization of resulting forces on a surface A due to absorption and specular reflection is shown in Figure 3. The normal vector \mathbf{n} in the figure gives the orientation of the surface A , and it is inclined an angle i_{sun} to the vector \mathbf{e}_{sun} which points in the direction of the Sun. For an absorbing surface, the impulse transferred is in the opposite direction as \mathbf{e}_{sun} . For a reflecting surface on the other hand, the impulse transferred is not generally in the opposite direction as \mathbf{e}_{sun} , and the impulse is also twice as large, due to the reflective rays. For a body that reflects a fraction γ of the incoming radiation, while it absorbs the remaining fraction of energy $(1 - \gamma)$, the total combined force is given as

$$\mathbf{f}_{sun}^s = -\frac{F_{sun}}{c} \cos i_{sun} A [(1 - \gamma) \mathbf{e}_{sun} + 2\gamma \cos i_{sun} \mathbf{n}] \quad (29)$$

where $F_{sun} = 1367 \text{ W/m}^2$ is the solar constant and c is the speed of light.

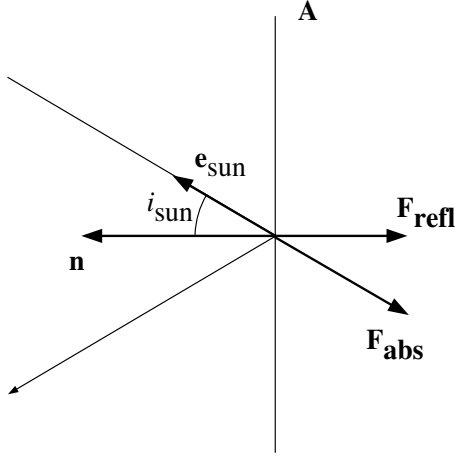


Figure 3: Disturbance forces due to solar radiation pressure for absorbing and reflecting surfaces.

5.1.3 The mass distribution of the Earth

If the Earth was a single point mass, the gravitational potential due to the conservative gravitational force could be derived from a gradient or scalar potential function $U(r) = -\mu/r$. However, the Earth is not a single point mass, but an oblate body with a nonhomogeneous mass distribution. Therefore, correction factors must be added based on the geographical position of the spacecraft, and the corrected potential of the Earth can be expressed as [17]

$$U(r, \phi, \lambda) = -\mu/r + B(r, \phi, \lambda)$$

where $B(r, \phi, \lambda)$ is a spherical harmonic expansion, ϕ is the geocentric latitude and λ is the geographical longitude of the spacecraft position. Denoting R_e as the mean equatorial radius of the Earth, the expansion can be expressed as

$$B(r, \phi, \lambda) = \frac{\mu}{r} \left\{ \sum_{n=2}^{\infty} \left[H_1 + \sum_{m=1}^n H_2 \right] \right\} \quad (30)$$

where

$$H_1 = \left(\frac{R_e}{r} \right)^n J_n P_n(\sin \phi)$$

$$H_2 = \left(\frac{R_e}{r} \right)^n (C_{nm} \cos m\lambda + S_{nm} \sin m\lambda) P_{nm}(\sin \phi)$$

which is the infinite series of the geopotential function at any point P outside of the Earth sphere where r , ϕ and λ are its spherical coordinates [15]. In (30), J_n are zonal harmonic coefficients, P_{nm} are Legendre polynomials of degree n and order m , $P_n = P_{n0}$, and C_{nm} and

S_{nm} are tesseral harmonic coefficients for $n \neq m$ and sectoral harmonic coefficients for $n = m$ [17]. Specifically, it should be noted that $J_n \equiv C_{n0}$. The associated Legendre polynomial P_{nm} is defined as [18]

$$P_{nm}(u) = (1 - u^2)^{\frac{m}{2}} \frac{d^m}{du^m} P_n(u)$$

It is seen from equation (30) that zonal harmonics depend only on latitude, not on longitude, and these coefficients are due to the oblateness of the Earth. The tesseral harmonics in (30) represents longitudinal variations in the Earth shape, and are generally smaller than zonal terms. A set of values for the J_n constants are given in Table 1 [19]. If the assumption of axial

n	J_n
2	$1082.6 \cdot 10^{-6}$
3	$-2.51 \cdot 10^{-6}$
4	$-1.60 \cdot 10^{-6}$

Table 1: Zonal harmonic coefficients

symmetry of the Earth is introduced, only zonal harmonics is needed. In addition, from Table 1 of zonal harmonics coefficients, it is seen that J_2 is considerably larger than the other J_n coefficients. If J_2 is the only zonal harmonic considered, the gravitational potential function can be approximated as [18]

$$U(r, \phi, \lambda) = \frac{\mu}{r} \left[-1 + \frac{1}{2} J_2 \left(\frac{R_e}{r} \right)^2 (3 \sin^2 \phi - 1) \right]$$

In the inertial reference frame,

$$\sin \phi = \frac{r_z}{|\mathbf{r}|} = \frac{r_z}{\sqrt{r_x^2 + r_y^2 + r_z^2}}$$

where \mathbf{r} is the vector pointing from the center of the Earth to the spacecraft. The gravitational force \mathbf{G} acting on the spacecraft is obtained from the gradient of the scalar potential as

$$\mathbf{G} = \mu \begin{bmatrix} -\frac{r_x}{r^3} + \frac{1}{2} J_2 R_e^2 \left(15 \frac{r_x r_z^2}{r^7} - 3 \frac{r_x}{r^5} \right) \\ -\frac{r_y}{r^3} + \frac{1}{2} J_2 R_e^2 \left(15 \frac{r_y r_z^2}{r^7} - 3 \frac{r_y}{r^5} \right) \\ -\frac{r_z}{r^3} + \frac{1}{2} J_2 R_e^2 \left(15 \frac{r_z^3}{r^7} - 9 \frac{r_z}{r^5} \right) \end{bmatrix} \quad (31)$$

and the J_2 gravity perturbation force \mathbf{f}_{grav}^b for the Earth is the latter terms in (31), i.e.

$$\mathbf{f}_{grav}^s = \frac{3}{2} \mu J_2 R_e^2 \mathbf{R}_i^s \begin{bmatrix} 5 \frac{r_x r_z^2}{r^7} - \frac{r_x}{r^5} \\ 5 \frac{r_y r_z^2}{r^7} - \frac{r_y}{r^5} \\ 5 \frac{r_z^3}{r^7} - 3 \frac{r_z}{r^5} \end{bmatrix}$$

5.1.4 Third-body perturbing forces

The gravitational potential of other bodies in the vicinity of the spacecraft can create perturbing forces and torques. For an Earth-orbiting spacecraft, the Sun and the Moon causes perturbing forces that can change the orbit parameters considerably. The Keplerian orbit models are derived from the two-body problem equation in (10), after a simplification of the general equation (9) due to the assumption the spacecraft and the orbited planet are the only elements present. If an extraction of the masses of the spacecraft and the Earth is performed on (9), the resulting accelerations are [13]

$$\frac{d^2 \mathbf{r}_1}{dt^2} = G \frac{m_2}{r_{12}^3} (\mathbf{r}_2 - \mathbf{r}_1) + G \sum_{j=3}^n \frac{m_j}{r_{1j}^3} (\mathbf{r}_j - \mathbf{r}_1) \quad (32)$$

$$\frac{d^2 \mathbf{r}_2}{dt^2} = G \frac{m_1}{r_{21}^3} (\mathbf{r}_1 - \mathbf{r}_2) + G \sum_{j=3}^n \frac{m_j}{r_{2j}^3} (\mathbf{r}_j - \mathbf{r}_2) \quad (33)$$

Subtraction of (32) from (33) results in the equation for the two-body problem in (10) with an additional perturbing acceleration due to the $n - 2$ perturbing bodies,

$$\frac{d^2 \mathbf{r}}{dt^2} + \frac{\mu}{r^3} \mathbf{r} = G \sum_{j=3}^n m_j \left(\frac{\mathbf{r}_{2j}}{r_{2j}^3} - \frac{\mathbf{r}_{1j}}{r_{1j}^3} \right)$$

where, as before, $\mathbf{r} = \mathbf{r}_2 - \mathbf{r}_1$ is the relative position of the two primary masses, and $\mathbf{r}_{1j} = \mathbf{r}_j - \mathbf{r}_1$ and $\mathbf{r}_{2j} = \mathbf{r}_j - \mathbf{r}_2$. Hence, the perturbing acceleration is

$$\mathbf{f}_{nbody}^s = \mathbf{R}_i^s \sum_{j=3}^n \mu_{pj} \left(\frac{\mathbf{r}_{2j}}{r_{2j}^3} - \frac{\mathbf{r}_{1j}}{r_{1j}^3} \right) \quad (34)$$

where $\mu_{pj} = Gm_j$ is the gravity constant for the j th perturbing body.

5.2 Perturbing torques

The resulting torque $\boldsymbol{\tau}_j^b$ on a spacecraft due to a perturbing force \mathbf{f}_j^b can be found from the relation [14]

$$\boldsymbol{\tau}_j^b = \mathbf{r}_c^b \times \mathbf{f}_j^b \quad (35)$$

where \mathbf{r}_c^b is the vector from the spacecraft center of mass to the line of action of the force. Hence, perturbing torques due to atmospheric drag, solar radiation, gravity variations and third body effects can be found by combining (35) with (28), (29), (31) and (34), respectively.

6 Simulations

To illustrate the impact of the perturbing forces and torques, simulation results for two spacecraft in a leader-follower formation are presented. It should be noted that only the effects of the gravity force and atmospheric drag are included in the simulations. The reason for this is that solar radiation and the third-body effects are dependent on the location of the Sun and other celestial bodies. The effect of these perturbations will therefore vary, depending on the orbit parameters and time of the year.

For simplicity of simulation, both spacecraft have mass $m = 1$ kg and their moments of inertia are $\mathbf{J} = \text{diag}([0.06, 0.06, 0.003])$ kgm². The leader spacecraft is assumed perfectly controlled in a circular orbit with inclination 22.5° and altitude 250 km, and with a constant attitude relative to the ECI frame. The follower spacecraft is located 10 m behind the leader in the along-track direction, with the same initial orbit velocity and attitude. For atmospheric drag, the spacecraft surface in the direction of motion of the spacecraft is chosen as 0.01 m², and the drag coefficient as $C_d = 1$. The simulations were performed using a Runge-Kutta ODE solver of order six and seven.

The position and velocity of the follower relative to the leader are shown in Figure 4. Similarly, the relative

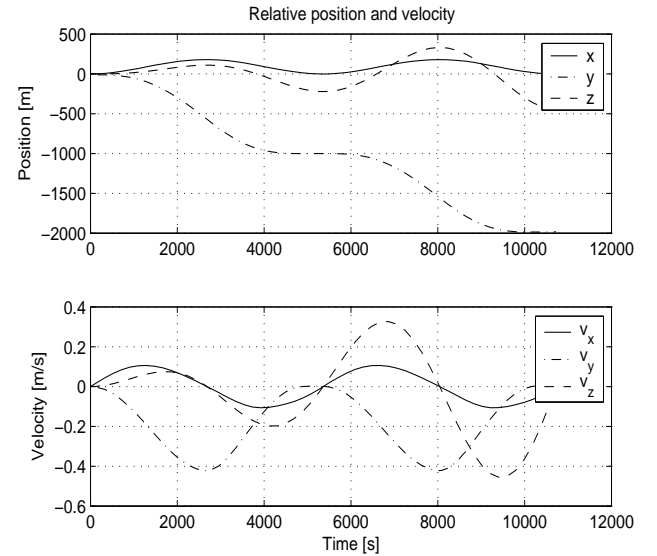


Figure 4: Relative position and velocity between spacecraft in formation.

attitude and angular velocity are presented in Figure 5. If no orbital perturbations were present, the relative position and attitude would be constant. Hence, the disturbance forces and torques can be seen from

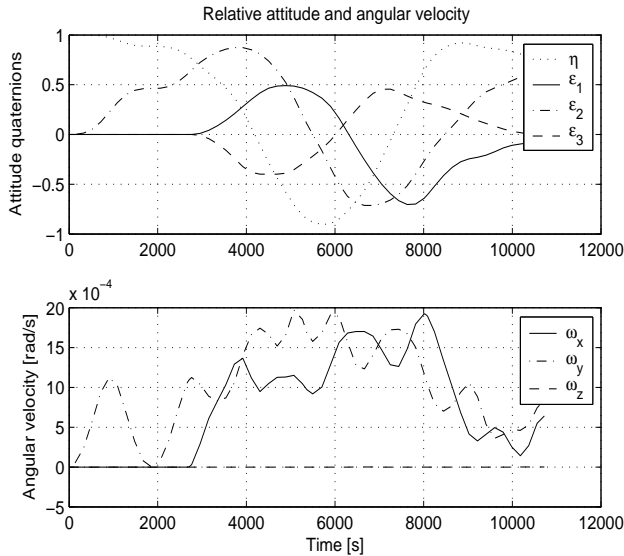


Figure 5: Relative attitude and angular velocity between spacecraft in formation.

the figures to have a large impact on the system states. From the results presented in Figure 4, it can be seen that the disturbance forces causes oscillations in relative position. This is due to the gravity force working on the follower. The force pulls the spacecraft downwards towards the Earth. However, as the follower moves below the leader, it has an orbital velocity corresponding to a higher orbit, and accordingly, the altitude increases. When it reaches the same altitude as the leader orbit, it is again drawn down towards the Earth, and the cycle repeats. Similar, the oscillations in the cross-track direction is due to gravity. Since the Earth is not a single point of mass, the follower will be drawn to the side with the largest gravitational pull. However, the main gravitational component will be towards the center of the Earth, so as the spacecraft moves to one side in cross-track direction, the gravitational force component in the opposite direction will pull it back again, and increased cross-track velocity will move it over to the other side. As with the altitude, this is also a cyclic behavior, however, the cross-track motion seems to be more unstable. The along-track distance between the spacecraft was however not oscillating, but constantly decaying. The main cause of this is probably the atmospheric drag, which has considerable effect at altitudes below 500 km. Hence, the along-track velocity of the follower is reduced. In addition, the oscillations in the other directions causes the satellite to have a longer flight path, and thus makes it lag behind.

The relative attitude was also seen to oscillate. All three body axes were influenced by the perturbations, they had the largest effect on the e_0 axis. This is due to the gravity force, which constantly tries to turn the follower towards the Earth, in accordance with the principle axis of inertia. In addition, gravity perturbations originating from oblateness of the Earth results in non-smooth attitude changes, as shown in the simulation results.

Regarding the perturbations due to solar radiation and third-body effects, these are not included in the simulations. It is however possible to get a notion of the impact of these perturbations. Since the orbital time is short, the location of other celestial bodies like the Sun and the Moon can be considered constant over one orbit period. If these bodies are located in the orbital plane, they will result in a change in orbit eccentricity for the follower. The perturbing force due to solar radiation will decelerate the follower as it moves towards the Sun, and accelerate it as it moves away from the Sun. If the Sun is located out of the orbit plane, the follower will experience a constant force away from the Sun. The third-body effects, which is the gravitational pull from other celestial bodies, will have the opposite effect on the follower compared to the solar radiation. Accordingly, the spacecraft will experience a pull towards these other celestial bodies.

7 Conclusion

In this paper, a nonlinear mathematical model of a leader-follower spacecraft formation in six degrees of freedom has been derived and presented. The model describes the relative translational and rotational motions of the spacecraft, and extends previous work by providing a more complete factorization, together with detailed information about the matrices in the model. In addition, mathematical models of orbital perturbations due to gravitational variations, atmospheric drag, solar radiation and third-body effects have been derived. Results from simulations of a leader-follower spacecraft formation have been presented to illustrate the effect of the orbital perturbations.

References

- [1] Hill, G. W., "Researches in lunar theory," *American Journal of Mathematics*, Vol. 1, No. 1, 1878, pp. 5–26.

- [2] Clohessy, W. H. and Wiltshire, R. S., "Terminal guidance system for satellite rendezvous," *Journal of Aerospace Sciences*, Vol. 27, No. 9, 1960, pp. 653–658.
- [3] Lawden, D., "Fundamentals of Space Navigation," *Journal of the British Interplanetary Society*, Vol. 13, No. 2, 1954, pp. 87–101.
- [4] Tschauner, J., "Elliptic Orbit Rendezvous," *AIAA Journal*, Vol. 5, No. 6, 1967, pp. 1110–1113.
- [5] McInnes, C. R., "Autonomous ring formation for a planar constellation of satellites," *AIAA Journal of Guidance, Control and Dynamics*, Vol. 18, No. 5, 1995, pp. 1215–1217.
- [6] Manikonda, V., Arambel, P. O., Gopinathan, M., Mehra, R. K., and Hadaegh, F. Y., "A model predictive control-based approach for spacecraft formation keeping and attitude control," *Proceedings of the American Control Conference*, San Diego, CA, 1999.
- [7] Yan, Q., Yang, G., Kapila, V., and de Queiroz, M., "Nonlinear dynamics and adaptive control of multiple spacecraft in periodic relative orbits," *Proceedings of the AAS Guidance and Control Conference*, Breckenridge, CO, 2000.
- [8] Wang, P. K. C. and Hadaegh, F. Y., "Coordination and control of multiple microspacecraft moving in formation," *Journal of Astronautical Sciences*, Vol. 44, No. 3, 1996, pp. 315–355.
- [9] Pan, H. and Kapila, V., "Adaptive Nonlinear Control for Spacecraft Formation Flying with Coupled Translational and Attitude Dynamics," *Proceedings of the Conference on Decision and Control*, Orlando, FL, 2001.
- [10] Naasz, B., Berry, M. M., Kim, H.-Y., and Hall, C. D., "Integrated orbit and attitude control for a nanosatellite with power constraints," *Proceedings of the AAS/AIAA Space Flight Mechanics Conference*, Ponce, Puerto Rico, 2003.
- [11] Ploen, S. R., Hadaegh, F. Y., and Scharf, D. P., "Rigid Body Equations of Motion for Modeling and Control of Spacecraft Formations - Part 1: Absolute Equations of Motion," *Proceedings of the American Control Conference*, Boston, MA, 2004.
- [12] Schaub, H. and Junkins, J. L., *Analytical Mechanics of Space Systems*, AIAA Education Series, American Institute of Aeronautics and Astronautics, Reston, VA, 2003.
- [13] Battin, R. H., *An Introduction to the Mathematics and Methods of Astrodynamics, Revised Edition*, AIAA Education Series, American Institute of Aeronautics and Astronautics, Reston, VA, 1999.
- [14] Egeland, O. and Gravdahl, J. T., *Modeling and Simulation for Automatic Control*, Marine Cybernetics, Trondheim, Norway, 2002.
- [15] Sidi, M. J., *Spacecraft Dynamics and Control*, Cambridge University Press, New York, 1997.
- [16] Fjellstad, O.-E., *Control of Unmanned Underwater Vehicles in Six Degrees of Freedom*, Ph.D. thesis, Department of Engineering Cybernetics, Norwegian University of Science and Technology, Trondheim, Norway, 1994.
- [17] Wertz, J. R., editor, *Spacecraft Attitude Determination and Control*, Kluwer Academic Publishers, London, 1978.
- [18] Montenbruck, O. and Gill, E., *Satellite Orbits. Models, methods, applications*, Springer-Verlag, Berlin, Germany, 2001, First edition, corrected second printing.
- [19] Roy, A. E., *Orbital motion, Fourth edition*, Institute of Physics Publishing Ltd, Bristol, UK, 2005.